

This article was downloaded by:[Bochkarev, N.]
On: 30 November 2007
Access Details: [subscription number 746126554]
Publisher: Taylor & Francis
Informa Ltd Registered in England and Wales Registered Number: 1072954
Registered office: Mortimer House, 37-41 Mortimer Street, London W1T 3JH, UK



Astronomical & Astrophysical Transactions

The Journal of the Eurasian Astronomical Society

Publication details, including instructions for authors and subscription information:
<http://www.informaworld.com/smpp/title~content=t713453505>

Nature of anomalous X-ray pulsars, soft gamma repeaters and radio pulsars with very long periods

I. F. Malov^a; G. Z. Machabeli^b

^a Pushchino Radio Astronomy Observatory, P.N. Lebedev Physical Institute, Russian Academy of Sciences, Moscow Region, Russia

^b Abastumani Astrophysical Observatory, Tbilisi, Georgia

Online Publication Date: 01 February 2006

To cite this Article: Malov, I. F. and Machabeli, G. Z. (2006) 'Nature of anomalous X-ray pulsars, soft gamma repeaters and radio pulsars with very long periods', *Astronomical & Astrophysical Transactions*, 25:1, 7 - 31

To link to this article: DOI: 10.1080/10556790600747474

URL: <http://dx.doi.org/10.1080/10556790600747474>

PLEASE SCROLL DOWN FOR ARTICLE

Full terms and conditions of use: <http://www.informaworld.com/terms-and-conditions-of-access.pdf>

This article maybe used for research, teaching and private study purposes. Any substantial or systematic reproduction, re-distribution, re-selling, loan or sub-licensing, systematic supply or distribution in any form to anyone is expressly forbidden.

The publisher does not give any warranty express or implied or make any representation that the contents will be complete or accurate or up to date. The accuracy of any instructions, formulae and drug doses should be independently verified with primary sources. The publisher shall not be liable for any loss, actions, claims, proceedings, demand or costs or damages whatsoever or howsoever caused arising directly or indirectly in connection with or arising out of the use of this material.

Nature of anomalous X-ray pulsars, soft gamma repeaters and radio pulsars with very long periods

I. F. MALOV*† and G. Z. MACHABELI‡

†Pushchino Radio Astronomy Observatory, P.N. Lebedev Physical Institute,
Russian Academy of Sciences, Pushchino, Moscow Region 142290, Russia

‡Abastumani Astrophysical Observatory, Al. Kazbegi Avenue 2a, 380060,
Tbilisi, Georgia

(Received 30 January 2006)

A brief review of the known models for the description of anomalous X-ray pulsars (AXPs) and soft gamma repeaters (SGRs) is given. A new model is proposed to explain the main properties of these objects on the basis of the concept of drift waves in the vicinity of the light cylinder of the neutron star with a surface magnetic field of about 10^{12} G. In the framework of this model, the rotation periods P , their derivatives dP/dt and the magnetic fields B in the regions of generation of emission observed in AXPs and SGRs are calculated. The intervals for these parameters are $P = 11\text{--}737$ ms, $dP/dt = 3.7 \times 10^{-16}\text{--}5.5 \times 10^{-12}$ and $\log B = 2.63\text{--}6.25$. A modulation with periods P could be observed in the sources under consideration. The magnetic fields at the neutron star's surface calculated in the framework of the dipole model for AXPs and SGRs have the same order ($\log B_s = 11.90$) as for normal radio pulsars. Pulsars of the types under consideration must have short periods ($P \approx 0.1$ s) and a small angle β between the rotation and magnetic axes ($\beta < 10^\circ$). It is expected that the fraction of these pulsars in the all-pulsar population must be of the order of 0.01. This estimate is in a good agreement with the known number of AXPs and SGRs. It is shown that the cyclotron radiation of electrons near the surface of a neutron star with a magnetic field of about 10^{12} G enables us to explain the observed quiescent X-ray emission of AXPs and SGRs. The pulsed emission is generated by the synchrotron mechanism near the light cylinder. Cataclysms on the neutron star can cause short gamma-ray bursts with a power exceeding the X-ray power by $2\gamma^2$ times. Here, γ is the Lorentz factor of the emitting electrons. It is shown that in the magnetar model the electron cyclotron line with an energy of about 1 MeV must be formed. Its detection provides good evidence for this model. The drift waves near the light cylinder can cause modulation of the emission with periods of the order of several seconds in radio pulsars as well. These periods explain the intervals between successive pulses observed in radio pulsars with long periods P between the observed pulses ($P > 4$ s). The model under consideration allows us to calculate the real rotation periods of host neutron stars. They are of the order of 1 s for the investigated objects. The magnetic fields at the surface of the neutron star are of the order of $10^{11}\text{--}10^{13}$ G and equal to the fields usual for normal radio pulsars.

Keywords: Anomalous X-ray pulsars; Soft gamma repeaters; Radio pulsars; Magnetic fields; Drift waves

*Corresponding author: Email: malov@ppao.psn.ru

1. Introduction

Two classes of astrophysical objects have been studied intensively during the last 10 years but their nature has been unclear up to now. These are anomalous X-ray pulsars (AXPs) and soft gamma repeaters (SGRs). Both classes are characterized by pulsed X-ray emission, and we can suggest that the central objects in these sources are isolated neutron stars because there is no evidence for the presence of secondary companions in all cases. The AXP group contains five confirmed sources and several candidates (see table 1 later). All data were taken from [1–8]. The main difference between AXPs and ‘normal’ X-ray pulsars is their monotonic slowing down with the derivatives dP/dt of the periods equal to about 10^{-13} – 10^{-10} . In addition, AXPs are characterized by the following features:

- (i) a fairly narrow range of periods (6–12 s);
- (ii) localization near the Galactic plane ($|b| = 0.35^\circ$);
- (iii) association with supernova remnants (SNRs), in the case of three objects;
- (iv) more stable X-ray fluxes than in pulsars belonging to binary systems, and a range of X-ray luminosities (10^{34} – 10^{36} erg s $^{-1}$) that is substantially less than for normal X-ray pulsars (10^{34} – 10^{38} erg s $^{-1}$);
- (v) a considerably softer spectrum than for other objects, which can usually be described by the sum of a black-body component with energy $kT \approx 0.35$ – 0.6 keV and a power-law component at higher energies with the exponent 2.5–4.0.

As for SGRs, there are four confirmed objects and one candidate (see table 1 later). Their pulse periods are in the same range as the periods of AXPs ($P = 5$ – 8 s). However, pulsed components are observed from these objects during quiet stages (SGR 1627-41 and 1806-20) only or vice versa when gamma-ray bursts occur (SGR 0525-66). Only SGR 1900 + 14 shows pulsed X-ray emission during all stages. The main distinctions of SGRs are episodic gamma-ray bursts with the total energy of each burst up to 10^{44} erg [5]. Sometimes there are more intensive flares. For example, SGR 1806-20 had a total (isotropic) flare energy of 2×10^{46} erg on 27 December 2004 [9].

If we use the known formula

$$B = 6.4 \times 10^{19} \left(P \frac{dP}{dt} \right)^{1/2} \quad (1)$$

obtained from the model in which the magnetodipole slows down, then the magnetic fields B at the surface of a neutron star in AXPs and SGRs must be 10^{14} – 10^{15} G, two orders of magnitude higher than fields in ‘normal’ pulsars. This was the reason why such objects were named magnetars. The second reason can be understood from the data in table 1. It is known that the main source of radio pulsar energy is connected with the losses of the rotation energy of a neutron star with the rate $dE/dt = I\Omega d\Omega/dt$. Here, I is the moment of inertia of a neutron star, $\Omega = 2\pi/P$ is its angular rotation velocity. However, if we take $I = 10^{45}$ g cm 2 , then energy losses for AXPs and SGRs, $dE/dt \approx 10^{33}$ erg s $^{-1}$, are much less than their X-ray luminosities. To avoid this difficulty it was suggested that X-radiation took its energy from a magnetic reservoir. Let us consider this possibility.

The total energy of such a reservoir is

$$E = \frac{B^2}{8\pi} \frac{4\pi R^3}{3} = 1.7 \times 10^{45} - 1.7 \times 10^{47} \text{ erg}, \quad (2)$$

where $R = 10$ km is the radius of the neutron star. The X-ray luminosity of SGR 1806-20 is 2×10^{35} erg s $^{-1}$. For $E = 10^{47}$ erg this source will exist for 10^4 years only. The lifetime of

normal radio pulsars is about 10^7 years. So, only one magnetar must be observed among 1000 known radio pulsars. This estimate is ten times less than the observed number. In fact, not all radio pulsars are observed. However, we can say the same about magnetars. We suggest here that the relative observed parts of these objects are equal to each other. Energy difficulties become more serious if we take into account the fact that SGR 1806-20 injects relativistic particles in the ambient SNR remnant with a rate of about 10^{37} erg s⁻¹ [10]. In this case, the magnetic reservoir will be exhausted after 360 years. However, the age of SGR 1806-20 is 1400 years.

To avoid this difficulty it is necessary to postulate the existence of magnetic fields $B \approx 10^{16}$ G inside a neutron star [11].

It is well known that the necessary stage to generate pulsar radio emission is the creation of electron–positron pairs:

$$\gamma + B \longrightarrow e^- + e^+ + B. \quad (3)$$

However, a gamma quantum will convert in very strong magnetic fields ($B \gg 10^{12}$ G) into two other gamma quanta [2]:

$$\gamma + B \longrightarrow \gamma_1 + \gamma_2 + B. \quad (4)$$

Therefore AXPs and SGRs must be radio-quiet objects. However, Shitov *et al.* [12] detected radio emission from SGR 1900 + 14 and Malofeev *et al.* [13] recorded pulsed radio signals from AXP 1E2259 + 586 and 1RXSJ1308 + 21.

So there are the following alternatives: either we do not understand how radio pulsars radiate or magnetic fields of AXPs and SGRs are much less than 10^{14} – 10^{15} G.

These difficulties compel some researchers to use the accretion model to explain the observable properties of AXPs and SGRs (see, for example, [14]). The accretion from ambient plasma gives an additional energy source for $B_s \approx 10^{12}$ G and it is not necessary to suggest super-strong magnetic fields. Moreover, the other mechanism describing the decrease in an angular moment appears, and large values of dP/dt can be explained without the fact that the magnetodipole slows down. In this case the braking index must differ from the magnetodipole value $n = 3$ (see, for example, [15]). In fact, the observations of SGR 1900 + 14 give $n = 0.2$ [12]. However, there is a number of difficulties in accretion models too. The accretion from the interstellar medium can provide luminosities $L \approx 10^{32}$ erg s⁻¹, much less than the observable values (see table 1 later). If accretion is connected with a relic disc, then the lifetime of this disc is very small and such accretion does not describe the observed slowing down of AXPs [16]. Plasma from a secondary component could explain the observed luminosities for the accretion rate $dM/dt \approx 10^{-11} M_\odot \text{ year}^{-1}$ [3]. However, there is no evidence of the presence of such components in AXPs or SGRs in all cases. An ambient plasma certainly exists around these objects, and accretion processes can play a role in their slowing down and evolution. However, the accretion models cannot explain the main properties of AXPs and SGRs.

2. Other models

- (i) Paczynski [17] and Usov [18] proposed the model of white dwarfs with $B \approx 10^8$ – 10^9 G. However, reasonable models of white dwarfs give $\log(dE/dt) \approx 36$. It is not sufficient to explain the injection of relativistic particles in ambient SNRs. Moreover, white dwarfs are required to have extremely short periods.
- (ii) The existence of strange stars [19, 20] is rather problematic, and possible models have not been worked out.

- (iii) Free precession of a neutron star can have periods of the order of 10 s [21, 22], but it is doubtful whether such long-lived precession is realized. Shaham [21] was the first researcher who said that the pulse period was not equal to the rotation period but was determined by another periodic process.

We believe also that the interval between two successive pulses is not equal to the rotation period.

In this report, we discuss a new model for describing the magnetar phenomenon using the usual values of magnetic fields at the surface of a neutron star, $B_s \approx 10^{12}$ G.

3. Basic features of the model

According to the theory [23–29], transverse electromagnetic waves can be generated in a relativistic electron–positron plasma, filling the magnetosphere of a neutron star. These waves easily escape the magnetosphere and reach the observer. Their frequency depends on the pulsar period and can be both in the radio range and at higher frequencies [23, 24]. The radiation generated in the magnetosphere must be separated into two parts: the eigenmodes and radiation in a one-particle approximation. The eigenmodes result from interference of the radiation by an ensemble of particles. In the second case, each particle of the ensemble is an independent source of radiation. In the first case, the wavelength λ is greater than the mean distance between the particles of the plasma with density n ($\lambda > n^{-1/3}$); in the second case, $\lambda < n^{-1/3}$.

As already mentioned above, a necessary stage of the magnetospherical processes is the formation of an electron–positron plasma near the neutron star surface. When $B_s \approx 10^{12}$ G, the particles lose their transverse momenta almost instantly (during the time $t < 10^{-15}$ s), so that their distribution function becomes one dimensional and has the form shown in figure 1. The plasma has three components:

- (i) the bulk of the plasma with density n_p and Lorentz factor γ_p ;
- (ii) a long tail with n_t and γ_t ;
- (iii) the primary beam with n_b and γ_b .

The general features of such a plasma have been described, for example, in [31, 32]. Since this plasma is not gyrotropic, there are three branches that propagate approximately along the magnetic field. We shall be interested only in the purely transverse t mode, with the spectrum

$$\omega_t = kc(1 - \delta), \quad (5)$$

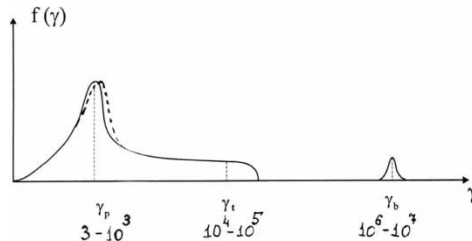


Figure 1. The distribution function of a relativistic plasma in a pulsar magnetosphere [30]. The broken curve is the positron distribution.

where

$$\delta = \frac{\omega_p^2}{4\omega_B^2\gamma_p^3}, \quad (6)$$

$$\omega_p^2 = \frac{4\pi n_p e^2}{m}, \quad (7)$$

$$\omega_B = \frac{eB}{mc}, \quad (8)$$

and the mixed potential–non-potential It mode, with the spectrum

$$\omega_{It} = k_\phi c \left(1 - \delta - \frac{k_\perp^2 c^2}{16\omega_p^2 \gamma_p} \right). \quad (9)$$

There are two basic mechanisms for the generation of the t and It eigenmodes: the resonance associated with the anomalous Doppler effect,

$$\omega - k_\phi v_\phi - k_x u_x = \frac{\omega_B}{\gamma_r}, \quad (10)$$

and the drift–Cherenkov resonance,

$$\omega - k_\phi v_\phi - k_x u_x = 0. \quad (11)$$

The resonance conditions (10) and (11) and spectrum (9) are written in the cylindrical coordinate system (figure 2). Here

$$u_x = \frac{cv_\phi \gamma_r}{\rho \omega_B}, \quad (12)$$

where ρ is the radius of curvature of the field line and γ_r is the Lorentz factor of the resonant particles.

These modes are generated within a small angle ($k_\perp/k_\phi \ll 1$) near the tangent to a curved field line in the outer part of the magnetosphere, where the field lines are distorted by the rotation. The waves propagate along the tangents to the field lines, enter a region between the closed and open field lines and leave the magnetosphere [33]. The generated t and It waves affect the resonant particles and transfer some of the energy to them. The wave field changes the particle distribution function. In particular, the beam and tail particles acquire non-zero pitch angles due to quasilinear diffusion. Since the motion of the particles is relativistic, synchrotron

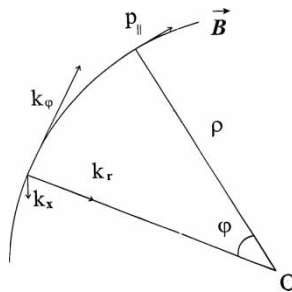


Figure 2. The coordinate system used in this paper.

radiation is generated in X-rays and gamma-rays [23, 24, 29, 34, 35]. The frequency of this radiation is

$$\nu = \nu_0 \frac{(1 - V^2/c^2)^{1/2}}{1 - (V \cos \alpha)/c}, \quad (13)$$

and its power is

$$P_\nu = P_{\nu_0} \frac{1}{1 - (V \cos \alpha)/c}, \quad (14)$$

where ν_0 is the frequency, P_{ν_0} is the power of the radiation in the rest frame of the particles ($V_{\parallel} = 0$) and α is the angle between the magnetic field in the region of wave generation and the line of sight to the observer. When $\alpha = 0$,

$$\nu = 2\gamma_r \nu_0, \quad P_\nu \approx 2P_{\nu_0} \gamma_r^2. \quad (15)$$

4. Mechanism for changing the field line curvature

As was shown in [36–38], together with t and lt waves, transverse electromagnetic drift waves can be generated in the magnetosphere. These waves propagate almost perpendicular to the magnetic field ($k_\phi/k_x \ll 1$). Using the smallness of the parameters $\gamma\omega/\omega_B \ll 1$ and $u_{dr}^2/c^2 \ll 1$ and assuming that $k_r = 0$, we can obtain the following dispersion relation for these waves:

$$\varepsilon_{\varphi\varphi} = \frac{k_x^2 c^2}{\omega^2 - k_\phi^2 c^2}, \quad (16)$$

where

$$\varepsilon_{\varphi\varphi} = 1 + \sum_i \frac{\omega_{pi}^2}{\omega} \int \frac{V_\varphi/c}{\omega - k_\phi v_\varphi - k_x u_x} \frac{\partial f}{\partial \gamma} d\left(\frac{p_\varphi}{mc}\right) \quad (17)$$

is the longitudinal–longitudinal component of the dielectric permittivity and $\omega_{pi}^2 = 4\pi n_{pi} e^2/m_i$. The summation over i in equation (17) is carried out over the kinds of particle ($i =$ electrons and positrons of the secondary plasma and electrons of the beam).

Let us assume that

$$\omega_0 = k_x u_x^b + k_\phi V_\varphi + a. \quad (18)$$

Here, u_x^b is the beam drift velocity, which can be fairly large for large γ_b . Partial integration of $\varepsilon_{\varphi\varphi}$ and summation over i taking into account equation (18) results in the expression [36]

$$1 - \frac{3\omega_p^2}{2\gamma_p^3 \omega^2} - \frac{\omega_p^2 k_x u_x^p}{2\omega^3 \gamma_p} - \frac{\omega_b^2}{\omega a \gamma_b^3} - \frac{\omega_b^2 k_x u_x^b}{\omega a \gamma_b} = \frac{k_\perp^2 c^2}{\omega^2}. \quad (19)$$

It can easily be shown that the third and fourth terms on the left-hand side of equation (19) are small. When $u_x^b/c \gg k_\phi/k_x$, it follows from equation (18) that

$$\omega_0 = \text{Re } \omega = k_x u_x^b \quad (20)$$

and, when $k_x^2 \ll \omega_p^2/c^2 \gamma_p^3$, the increment will be

$$\Gamma = \text{Im } \omega = \text{Im } a \approx \left(\frac{n_b}{n_p}\right)^{1/2} \frac{\gamma_p^{3/2}}{\gamma_p^{1/2}} k_x u_x^b. \quad (21)$$

This increment is quite small; when $\gamma_b \approx 10^6$ and $\gamma_p \approx 10$, we obtain $\Gamma \approx 10^{-4} \omega_0$. However, since the wave is almost perpendicular to the magnetic field, it propagates around the magnetosphere and is located in the generation region for a long time. As a result, the amplitude of

the drift waves can increase to large values [36] via the kinetic energy of the particles moving along the magnetic field with velocity V_φ . These particles cross the generation region in a short time (less than 10^{-2} s), but other particles enter the region, while the wave remains in nearly the same place. Its amplitude increases until nonlinear processes (in particular, induced scattering by the particles) begin to transfer wave energy to the region with the minimum wave number k (i.e. the maximum wavelength λ_{\max}). The value of λ_{\max} depends on the transverse size of the magnetosphere, which can be identified with the radius of the light cylinder, $r_{\text{LC}} = cP/2\pi$.

The drift waves are stabilized owing to the rotation of the neutron star and the permanent injection of relativistic particles in the region of their generation.

The electric field vector of the low-frequency drift wave propagating perpendicular to the pulsar magnetic field is directed along this field $E(E_\varphi, 0, 0)$, and its magnetic field is directed along the axis $r: B(0, 0, B_r)$. It follows from the Maxwell equation

$$\text{curl } \mathbf{E} = -\frac{1}{c} \frac{\partial \mathbf{B}}{\partial t} \quad (22)$$

that

$$B_r = \frac{E_\varphi kc}{\omega}. \quad (23)$$

As $kc/\omega \approx kc/k_x u_x \gg 1$, then $B_r \gg E_\varphi$. Thus, mainly the r component of the magnetic field is perturbed in this region, and this effect leads to a change in the magnetic field line curvature. In a Cartesian coordinate system we have

$$\frac{dy}{dx} = \frac{B_y}{B_x}, \quad (24)$$

and the curvature of any field line is determined by the formula

$$K = \frac{1}{\rho} \left[1 + \left(\frac{dy}{dx} \right)^2 \right]^{-3/2} \frac{d^2 y}{dx^2}. \quad (25)$$

Using the equation

$$\text{div } \mathbf{B} = 0 \quad (26)$$

and the condition $k_r = 0$, we obtain in cylindrical coordinates

$$K = \frac{B_\varphi}{B_r} - \frac{B_\varphi^2 \partial B / \partial \varphi}{B^3 r}. \quad (27)$$

The change in

$$K = (B_\varphi^2 + B_r^2)^{1/2} \approx B_\varphi \left(1 + \frac{B_r^2}{2B_\varphi^2} \right) \quad (28)$$

is negligibly small, and

$$K \approx \frac{1 - k_\varphi r B_r / B_\varphi}{r}. \quad (29)$$

If $k_\varphi r \gg 1$, the change in K may be significant. As radiation is emitted along a tangent to the local direction of the magnetic field, the change in its curvature leads to a change in the radiation direction.

5. The model under consideration

Let us consider the case of small angles β between the rotation axis of a neutron star and its magnetic moment vector μ (figure 3). Radiation from such an object can be recorded during almost all its period. If a disturbance of field lines takes place owing to the interaction with the drift waves, an additional emission appears. This part of the emission missed the line of sight before such an interaction (the broken line in figure 3). Now it goes to the observer (the solid line in figure 3). This part of the emission has a pulsed character. Its period is $P_{\text{dr}} = 2\pi/\omega_{\text{dr}}$, and such an emission explains the main properties of magnetars.

It is worth noting that thermal emission from the surface of a neutron star or from its polar cap can give a contribution to the continuous component of observed radiation. If the distribution of such an emission has a spatial maximum, we shall observe a modulation in the received signal with the rotation period of the neutron star.

Let us estimate the thermal luminosity and the non-thermal (synchrotron) luminosity for such a star. If we suggest that the polar cap has a temperature of 10^7 K due to bombardment by the secondary positrons, then its luminosity is

$$L_{\text{th}} = \pi r_p^2 \sigma T^4 = \frac{2\pi^2 \sigma R^3 T^4}{cP}. \quad (30)$$

Here, r_p is the radius of the polar cap and σ is the Stefan–Boltzmann constant. We obtain, for $P \approx 0.1$ s, $L_{\text{th}} = 3.8 \times 10^{33}$ erg s $^{-1}$.

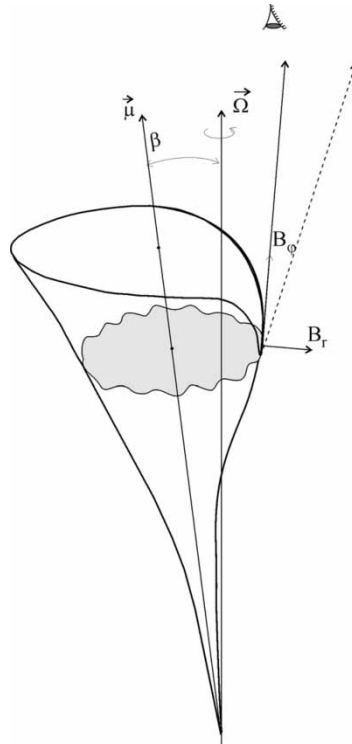


Figure 3. Scheme of the model.

We can use the results of Malov and Machabeli [39] to calculate the synchrotron luminosity:

$$L = \frac{3^{1/2} \pi^{7/2} e}{32 m^{1/2} c^{3/2}} \frac{I \gamma_b^{3/2} dP/dt}{P^{7/2} \gamma_p^2}, \quad (31)$$

where I is the moment of inertia of a neutron star. We obtain, for $\gamma_b \approx 10^6 - 10^7$, $P = 0.1 - 0.2$ s, $dP/dt \approx 10^{-13} - 10^{-12}$ and $\gamma_p = 3 - 10$, $L_s \approx 10^{33} - 3 \times 10^{35}$ erg s $^{-1}$.

As for the main part of emission it is very important to know the location of its generation. If this region is located at very large distances from the surface of a neutron star, as we suggest in our model, the observer can see either the continuous emission only or this emission and emission modulated by the drift waves together. Now we consider the modulated part only.

Let us calculate the period of the drift waves. This period determines the interval between observed pulses:

$$P_{dr} = \frac{2\pi}{\omega_{dr}} = \frac{2\pi}{k_x u_x^b} = \frac{\lambda_{dr}}{u_{dr}^b}. \quad (32)$$

As we noted earlier, the maximum value of the wavelength was $\lambda_{max} = cP/2\pi$. In this case, taking for the curvature radius value $\rho = cP/2\pi$, we can write [40]

$$P_{dr}^{max} = \frac{eBP^2}{4\pi^2 mc \gamma_b}. \quad (33)$$

To obtain the observed value of the pulse period $P_{dr}^{max} \approx 10$ s we must fulfil the following equality:

$$BP^2 = 22.45 \text{ G s}^2. \quad (34)$$

Here we put $\gamma_b = 10^6$. If magnetic field is dipolar and its value at the surface of a neutron star is $B_s \approx 10^{12}$ G, then $B \approx 1000$ G at distances $r \approx 1000R$. The rotation period of such a star must be equal to $P = 0.15$ s according to the equality (34). Hence, the ‘normal’ magnetic fields of neutron stars can explain the observed periods $P_{obs} \approx 10$ s of magnetars if there are drift waves in the vicinity of the light cylinder. If the rotation period $P = 2$ s and the surface magnetic field $B_s = 10^{12}$ G, then $P_{dr}^{max} \approx P \approx 2$ s at the light cylinder. In this case the drift of subpulses can be observed [36].

We made the calculations for the maximum value of the drift wave period. In fact, the spectral energy of the drift waves with smaller periods is much less than that of the mode with the period $P = P_{dr}^{max}$.

The equality (33) gives the possibility of linking the observed derivative $(dP/dt)_{dr}$ of the period with the real rate dP/dt of the slowing down of the neutron star rotation:

$$\left(\frac{dP}{dt}\right)_{dr} = \frac{eBP dP/dt}{2\pi^2 mc \gamma_b}. \quad (35)$$

We have for the considered values of the parameters

$$\frac{dP}{dt} = 7.48 \times 10^{-3} \left(\frac{dP}{dt}\right)_{dr}. \quad (36)$$

So, $(dP/dt)_{dr} \approx 10^{-10}$ will be observed if $dP/dt = 7.48 \times 10^{-13}$. This value is usual for a number of young radio pulsars such as the Crab pulsar.

The dependences (33) and (35) show that, if there are jumps in the rotation period and its derivative (‘glitches’), then similar jumps must be observed in the values of P_{dr} and (dP_{dr}/dt) as well.

It is very important to estimate the braking index n of investigated objects in the framework of our model. This parameter is determined by the formula

$$n = \frac{\Omega d^2 \Omega / dt^2}{(d\Omega / dt)^2} \quad (37)$$

or

$$n = 2 - \frac{P d^2 P / dt^2}{(dP / dt)^2}. \quad (38)$$

The last formula was used to calculate the n value cited for SGR 1900 + 14 in Section 1. Using equation (33) we can calculate P , dP / dt and $d^2 P / dt^2$ and obtain

$$n = 3 - \frac{2P_{dr}(d^2 P / dt^2)_{dr}}{(dP / dt)_{dr}^2}. \quad (39)$$

We know of only one magnetar (SGR 1900 + 14) with the measured value of $d^2 P / dt^2$ [12]. Shitov *et al.* [12] gave the following results obtained during the period 12 December 1988–30 July 1999:

$$\begin{aligned} P &= 5.16 \text{ s}, \\ \frac{dP}{dt} &= 1.23 \times 10^{-10}, \\ \frac{d^2 P}{dt^2} &= 0.53 \times 10^{-20}. \end{aligned}$$

These values give $n = -0.61$. A similar value of the braking index was obtained for radio pulsars with short periods ($P < 0.1$ s) [41]. It requires special slowing-down mechanisms and cannot be explained by the magnetodipole braking described by the value $n = 3$. Hence we cannot use the magnetodipole model for calculating the magnetic fields in AXPs and SGRs.

Values of $d^2 v / dt^2$ for 1RXS 1708-4009 and 1E2259.1 + 586 [42] do not describe the intrinsic braking mechanism but characterize post-glitch recovery.

Let us estimate now the losses of the rotation energy of the neutron star:

$$\frac{dE}{dt} = \frac{4\pi^2 I dP / dt}{P^3}. \quad (40)$$

The calculated values of $P = 0.15$ s and $dP / dt = 7.5 \times 10^{-13}$ lead to $dE / dt \approx 10^{37}$ erg s⁻¹. Here we take the value $I = 10^{45}$ g cm² for the moment of inertia. The obtained losses are quite enough to explain observed the X-ray luminosities L_X of AXPs and SGRs (table 1) and the rates of ejection of relativistic particles in ambient SNRs.

The total rotation energy $E = I\Omega^2 / 2$ for the same values of the parameters is approximately equal to 10^{48} erg. Such a reservoir can provide 10^4 gamma-ray bursts with energies of about 10^{44} erg.

Taking into account two peculiarities of the objects under consideration, namely the first group with small angles β between the rotation and magnetic axes ($\beta < 10^\circ$) and the second group with small rotation periods ($P \lesssim 0.1$ s), we can estimate the expected number of AXPs and SGRs among the known radio pulsars. The first group contains about 10% of the whole pulsar population, if neutron stars are formed with an arbitrary angle β . The second group consists of approximately a tenth of all pulsars. So, we can expect that there are about 1% of AXPs and SGRs in the whole sample of 1500 radio pulsars. In fact, we observe about 15 such objects.

So, our model can describe all the main characteristics of the known AXPs and SGRs.

Table 1. Observed parameters of the well-studied AXPs and SGRs.

Number	Source	P_{obs} (s)	$(dP/dt)_{-11}$	$\log[L_X(\text{erg s}^{-1})]$	f_{pl} (%)	W_X/P_{obs}
<i>AXPs</i>						
1	4U0142 + 61	8.69	0.196	34.52	≈88	0.53
2	1E1048-5937	6.45	≈3.81	34.53	≈80	0.44
3	RXS1709-4009	11.00	1.86	35.83	≈73	0.67
4	1E1841-045	11.77	4.16	35.36	100	0.64
5	1E2259 + 586	6.98	0.0483	35.00	≈50	0.48
6	XTEJ1810-197	5.54	1.15	36.20	≈70	0.41
7	AXJ1845.0-0258	6.97		34.70		
<i>SGRs</i>						
1	SGR1806-20	7.48	0.083	35.30	≈2.5	0.65
2	SGR1900 + 14	5.16	11	34.48	≈5	0.38
3	SGR 0526-66	8.1		36-37		
4	SGR 1627-41	6.4?		≈35		

We can calculate some parameters of each source under consideration using the observed values of the periods, their derivatives, the pulse widths W_X , the pulsed part f_{pl} of the emission (table 2) and the formula for the synchrotron luminosity [43] as the third equation (see equation (31)).

Radio pulsars with the recorded X-ray pulsed emission are characterized by the mean value of the parameter $\gamma_b^{3/2}/\gamma_p^2 = 4.37 \times 10^8$ [15]. We take this value for our sample. The estimate for the synchrotron luminosity can be obtained for AXPs and SGRs from L_X , if we take into account the beam width and the percentage of pulsed emission:

$$L = \left(\frac{W_X}{P_{\text{obs}}} \right)^2 f_{\text{pl}} L_X. \quad (41)$$

Then we can calculate P , dP/dt and B from the system (35), (36) and (41):

$$P(\text{s}) = 8.32 \times 10^{-2} \left(\frac{(dP/dt)_{\text{obs}/-11}}{(L_X)_{34} (W_X/P_{\text{obs}})^2 P_{\text{obs}} f_{\text{pl}}} \right)^{2/5}, \quad (42)$$

$$\frac{dP}{dt} = \frac{P(dP/dt)_{\text{obs}}}{2P_{\text{obs}}}, \quad (43)$$

$$B(\text{G}) = \frac{22.45 P_{\text{obs}}}{P^2}. \quad (44)$$

Table 2. Calculated parameters of AXPs and SGRs.

Number	Source	P (ms)	dP/dt ($\times 10^{-15}$)	\log [$L(\text{erg s}^{-1})$]	\log [$B(\text{G})$]	$\log[(dE/dt)$ ($\text{erg s}^{-1})$]	$-\log \eta$	\log [$B_s(\text{G})$]
<i>AXPs</i>								
1	4U0142 + 61	19.81	2.23	33.91	5.70	37.06	3.15	11.60
2	1E1048-5937	87.22	2.58	33.72	4.28	37.18	3.46	12.10
3	RXS1709-4009	11.84	10	35.35	6.25	38.38	3.03	11.46
4	1E1841-045	22.41	40	34.97	5.72	38.14	3.17	11.77
5	1E2259 + 586	10.75	0.372	34.06	6.13	37.07	3.01	11.22
6	XTEJ1810-197	13.78	14	35.27	5.82	38.33	3.06	11.24
7	1RXSJ130848.6 + 212708	737	482	30.75	2.63	34.68	3.93	13.24
<i>SGRs</i>								
1	SGR1806-20	25.60	1.42	33.32	5.41	36.52	3.20	11.64
2	SGR1900 + 14	520	5545	32.34	2.63	36.19	3.85	12.79

We put in (42) and further $(dP/dt)_{\text{obs}/-11} = (dP/dt)_{\text{obs}/10}$, $(L_X)_{34} = L_X/10^{34}$ and so on, and assume that $I = 10^{45} \text{ gcm}^2$ and $\gamma_b = 10^7$.

The results of our calculations can be seen in table 2.

The dependence of L_X (table 1) on dE/dt from table 2,

$$\log L_X = (0.60 \pm 0.28) \log \left(\frac{dE}{dt} \right) + 13.08 \pm 7.52, \quad (45)$$

and the high correlation coefficient ($K \approx 0.8$) between L_X and dE/dt show that losses of the rotation energy can be the real energy source of the X-ray emission in AXPs and SGRs. The relationship between the X-ray luminosity and dE/dt for 41 radio pulsars [44] has rather a different form

$$\log L_X = (1.33 \pm 0.09) \log \left(\frac{dE}{dt} \right) - 15.28 \pm 3.29. \quad (46)$$

However, in these objects the rotation energy losses is the main source of their X-ray emission as well.

It is worth noting that the values of dE/dt in table 2 are higher than $10^{37} \text{ erg s}^{-1}$ for many objects and they are sufficiently high to explain the observed injection of relativistic particles into ambient SNRs. Moreover the objects in our sample and radio pulsars with X-ray emission have, as a rule, short periods. For AXPs and SGRs in table 2, $\langle P \rangle = 161 \text{ ms}$ and, for 41 pulsars from [44], $\langle P \rangle = 128 \text{ ms}$. The distributions of periods for these objects are identical as well. Indeed, among 41 sources from [44] there are pulsars with periods P from milliseconds to dozens of milliseconds (1.56–89 ms) and with $P = 0.1\text{--}0.53 \text{ s}$. Table 2 contains also AXPs and SGRs with $P \approx 10 \text{ ms}$ (1E2259 + 586 and RXS 1709-4009), with periods of the order of tens of milliseconds (1E1048-5937) and with $P > 0.1 \text{ s}$ (1RXS130848.6 + 212708 and SGR 1900 + 14).

The positions of AXPs and SGRs on the $dP/dt - P$ diagram (figure 4) are shown as full circles. The $dP/dt - P$ relationship can be presented in the following form:

$$\log \left(\frac{dP}{dt} \right)_{-15} = (1.48 \pm 0.43) \log[P(\text{s})] + 3.19 \pm 0.65, \quad (47)$$

with the correlation coefficient $K = 0.79 \pm 0.23$.

A similar dependence can be obtained for short-period radio pulsars recycled in binary systems.

The new pulsar catalogue [46] contains 94 pulsars with $dP/dt > 0$ and $P < 0.1$, and 23 sources of these belong to objects such as the Crab pulsar and the Vela pulsar (PSR B0531 + 21 and PSR B0833-45) with $P > 30 \text{ ms}$ and $(dP/dt)_{-15} > 1$. Excluding these from the considered sample we obtain

$$\log \left(\frac{dP}{dt} \right)_{-15} = (1.28 \pm 0.21) \log[P(\text{s})] - 1.53 \pm 0.46, \quad (48)$$

$$K = 0.59 \pm 0.10.$$

The $dP/dt(P)$ dependence coincides with equation (47) and shows the similarity of objects in these two samples.

The braking index n determined by the equation

$$\frac{d\Omega}{dt} = k\Omega^n, \quad (49)$$

is near to zero for AXPs and SGRs. This means that some other braking mechanisms operate in these objects [41, 47–50].

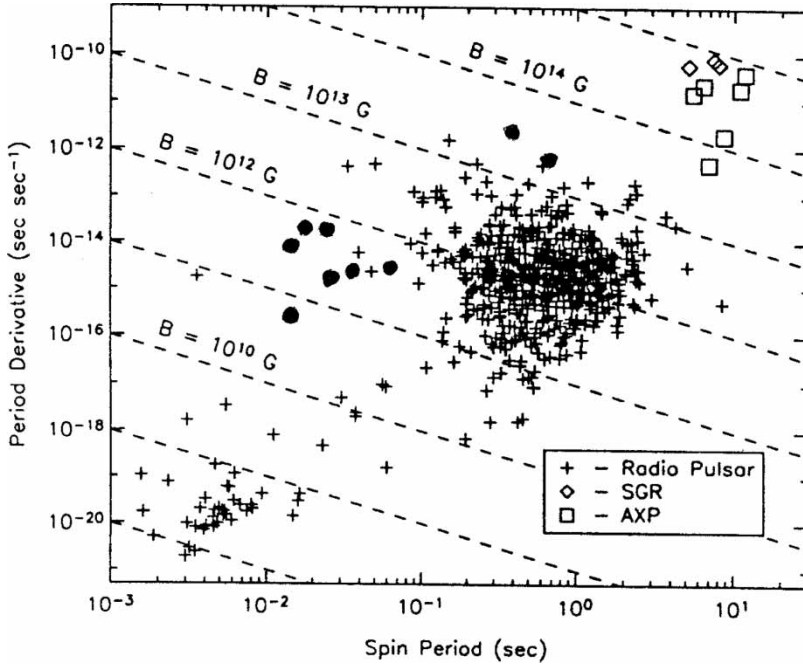


Figure 4. Locations of AXPs and SGRs on the $dP/dt - P$ diagram in the framework of our model (full circles) and the magnetar model [45].

We must note, however, that the calculated values of dP/dt for AXPs and SGRs differ by five orders of magnitude from those for radio pulsars with short periods. This difference can mean that two classes of objects followed different ways of evolution to the modern stages. For example, recycling of pulsars for periods up to milliseconds occurred and decreases in their period derivatives and magnetic fields. The braking mechanism can be connected in both types of object with ambient media and with the realization of a ‘propeller’ regime [48, 50].

The efficiency of the transformation of the rotation energy of AXPs and SGRs into pulsed X-ray emission, given by

$$\eta = \frac{L}{dE/dt} = \frac{LP^3}{4\pi^2 I dP/dt}, \quad (50)$$

can be written in the following form:

$$\eta = 3.41 \times 10^6 \frac{3^{1/2} \pi^{3/2} e}{m^{1/2} c^{3/2} P^{1/2}} = 10^{-4} P^{-1/2}. \quad (51)$$

This dependence is similar to that for 27 pulsars with $P < 0.1$ s [51]:

$$\begin{aligned} \log \eta &= (-1.04 \pm 0.49) \log P - (6.99 \pm 1.03), \\ K &= -0.40 \pm 0.19. \end{aligned} \quad (52)$$

However, the efficiency for AXPs and SGRs is 1000 times higher than for radio pulsars.

The values of magnetic field in the region of observed X-ray emission have been calculated without any additional assumptions about its structure and the value of B_s at the surface of a neutron star. If emission is generated at the light cylinder and this field is dipolar, we can

estimate B_s (table 2):

$$\log B_s = 11 + \log B + 3 \log P. \quad (53)$$

The mean value $\langle \log B_s \rangle = 11.90$ is equal to the strength of the surface field for normal radio pulsars.

One of the basic problems in the AXP and SGR investigations is the possibility of the generation of radio emission by these objects. Here, we have used the model of cyclotron instability [26]. In this model, the frequency of generated transverse waves is

$$\omega = \frac{4\omega_B^3 \gamma_p^3}{\omega_p^2 \gamma_b}. \quad (54)$$

Let us estimate the distance where emission at 100 MHz is generated. For the dipole magnetic field,

$$\frac{r}{R_*} = \left(\frac{e^2 B_s^2 \gamma_p^4 P}{\pi^2 m^2 c^2 \gamma_b^2 \nu} \right)^{1/6} = \left(3.1 \times 10^{37} \frac{B_{12}^2 \gamma_p^4 P}{\gamma_b^2 \nu} \right)^{1/6} = 10^3 (B_{12}^2 P)^{1/6}. \quad (55)$$

Here we suggest that $\gamma_b = 10^7$, $\gamma_b^{3/2} / \gamma_p^2 = 4.37 \times 10^8$,

$$n_b \gamma_b = 2n_p \gamma_p \quad (56)$$

and

$$n_b = \frac{B}{ecP}. \quad (57)$$

It is evident that $r \approx r_{LC} = cP/2\pi$ for 1RXSJ130848.6 + 212708 and SGR 1900 + 14 only. It is worth noting that these objects are recorded as radio emitters [12, 13]. For other AXPs and

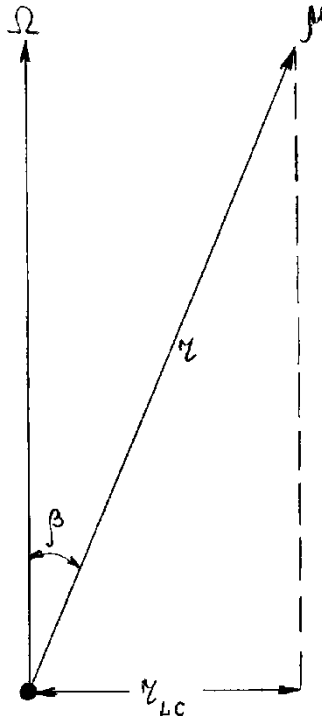


Figure 5. Scheme illustrating the possibility of emission generation at distances $r > r_{LC}$.

SGRs, $r/r_{\text{LC}} = 3 - 9$. However, the generation of radio emission is possible in these sources as well, because the scale of their magnetospheres can be much more than r_{LC} (figure 5). In our model, $\beta < 10^\circ$; hence r can be more than $6r_{\text{LC}}$.

The increment in the cyclotron instability

$$\Gamma_c = \frac{\pi \omega_p^2}{\omega \gamma_T}, \quad (58)$$

can be rather high ($\Gamma_c \Delta r/c \gg 1$) to provide the required intensification of the waves. Here γ_T is the width of the distribution function of resonant particles. We believe that those are the particles of the primary beam with $\langle \gamma_b \rangle = 10^6$ and $\gamma_T = 100$.

Table 2 shows that, for the known AXPs and SGRs, $P = 10 - 740$ ms, $dP/dt = 3.7 \times 10^{-16} - 5.5 \times 10^{-12}$ and $\log B = 2.63 - 6.25$.

The surface magnetic fields of AXPs and SGRs ($\langle \log B_s \rangle = 11.90$) are equal on the average to the fields of normal radio pulsars.

In our model we can expect a modulation of observed emission with the rotation period ($P \approx 0.1$ s). The detection of such modulation will be good evidence of the importance of this model.

6. Quiescent X-ray emission

What is the origin of the quiescent X-ray emission and gamma-ray bursts? It is well known that near the surface of a neutron star the process described by equation (3) takes place, and newly generated electrons and positrons populate the Landau levels. Let us consider the following question: what is the frequency range corresponding to radiation near the surface?

The frequency ν in the observer's coordinate system depends on the frequency ν_0 in the system where $V_{\parallel} = 0$ [52] and it is determined by equation (13).

If the Lorentz factor of emitting particles is $\gamma = (1 - V^2/c^2)^{-1/2} \gg 1$, and the angle α is small, equation (13) can be presented in the following form:

$$\nu = \frac{2\nu_0}{1/\gamma + \alpha^2\gamma}. \quad (59)$$

If $\alpha^2\gamma \ll 1/\gamma$, then

$$\nu \approx 2\nu_0\gamma. \quad (60)$$

In the opposite case,

$$\nu \approx \frac{\nu_0}{\gamma}. \quad (61)$$

For

$$1 \lesssim \alpha^2\gamma \lesssim 10, \quad (62)$$

and $B \approx 10^{12}$ G, the electron cyclotron frequency

$$\nu_0 = \frac{eB_s}{2\pi mc}, \quad (63)$$

is in the soft X-ray range (1–10 keV) in the observer's system. This emission can penetrate through the e^\pm magnetosphere and arrive at the observer. The diapason of angles α can be very wide, and the distribution function of the emitting particles is not monoenergetic; therefore the resulting spectrum must be wide too.

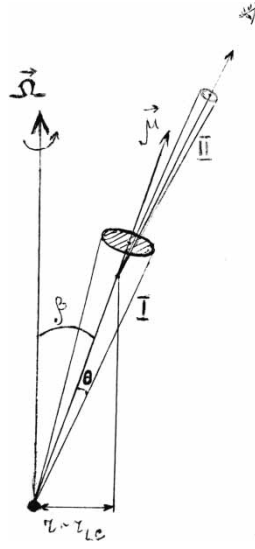


Figure 6. The cones of X-ray emission in AXPs and SGRs.

The magnetic field of a neutron star decreases with increasing distance, and the frequency coincides with one of the Landau harmonics [53]:

$$\varepsilon_m - \varepsilon_n = \frac{p_{\perp m}^2 - p_{\perp n}^2}{2m_e} = h\nu_0 S, \quad (64)$$

$$S = m - n = \pm 1, \pm 2, \dots,$$

near the surface only. Lines corresponding to such harmonics have been detected in fact [54]. There have been some attempts (see, for example, [55]) to interpret them as the absorption lines of non-relativistic protons in magnetic fields of about 10^{14} – 10^{15} G. However, according to Ho *et al.* [56], vacuum polarization effects suppress not only proton cyclotron lines but also any spectral features due to bound species. Therefore spectral lines or features in radiation are much more difficult to observe when the magnetic field B_s of the neutron star is greater than 10^{14} G. Moreover in this case the electron cyclotron lines in the range near 1 MeV must be observed. Their detection will be good evidence for the magnetar model. In our model, such lines must not be observed in the spectra of AXPs and SGRs.

The emission beam of relativistic particle has the width $\theta \approx 1/\gamma$ [57].

We believe that this near-surface emission is the main part of the observed quiescent X-ray radiation of AXPs and SGRs. As we stated, near the light cylinder, pulsed emission was generated. So, we must observe two emission cones, as shown in figure 6.

7. Irregular gamma-ray bursts

If for any reason (e.g. star quakes) the cone I changes its position so that the angle α becomes very small ($\alpha^2 \gamma^2 \lesssim 1$) for a short time, then the frequency can achieve a high value ($\nu \approx 2\gamma\nu_0$). This frequency can be in the gamma-ray range. Particles with different Lorentz factors can take part in this process, and the observed spectrum must be wide. The transformation of the power into the observer's system is described by equation (14) and, for $\alpha \rightarrow 0$, P_ν increases drastically ($P_\nu \approx 2P_{\nu_0}\gamma^2$). So, the power in the gamma-ray range can be $2\gamma^2$ times higher

than in X-ray range. If the X-ray power is $10^{36} \text{ erg s}^{-1}$, the Lorentz factor must be $\gamma \approx 10^4$ to provide a gamma-ray burst with a power of $10^{44} \text{ erg s}^{-1}$. In the traditional model, this energy characterizes the tail of the distribution function for the secondary particles (figure 1). To achieve the power $2 \times 10^{46} \text{ erg s}^{-1}$ as in SGR 1806-20 we must put $\gamma \approx 10^5$. There are such particles in the tail of the secondary plasma as well.

8. Radio pulsars with very long periods

Recently, radio pulsars with long periods were discovered (see table 3 later). They must be in the radio-quiet zone. PSR J2144-3933, discovered in 1999 [58], has the longest (8.5 s) pulse period among the known radio pulsars. PSR J2144-3933 is distinguished by some other characteristics. It has the lowest spin-down luminosity ($dE/dt \approx 3.2 \times 10^{28} \text{ erg s}^{-1}$) of any known pulsar. The beaming fraction (i.e. the fraction of the celestial sphere swept across by the beam) is also the smallest, $W_{10}/P \approx 1/300$. On the other hand, PSR J1847-0130 [59] and PSR J1814-1744 [60] are isolated radio pulsars having the largest inferred surface dipole magnetic fields B_s yet seen in the population: $9.4 \times 10^{13} \text{ G}$ and $5.5 \times 10^{13} \text{ G}$, respectively. These pulsars show apparently normal radio emission in a regime of magnetic field strength ($B_s > B_{\text{cr}} = 4.4 \times 10^{13} \text{ G}$) where some models predict that no emission should occur.

No model explaining the phenomenon of radio emission from all these pulsars and all the special properties of PSR J2144-3933 exists at present.

We proposed a model [61] that provides a natural explanation of the peculiarities of pulsars under consideration. We believe that the observed interval between successive pulses is not equal to the rotation period but is determined by the period of drift waves as in AXPs and SGRs. The variation in the field line curvature can be estimated as

$$\frac{\Delta\rho}{\rho} \approx k_\varphi r \frac{\Delta B_r}{B_\varphi}. \quad (65)$$

It follows that even the drift wave with a modest amplitude $B_r \approx \Delta B_r \approx 0.01 B_\varphi$ alters the field line curvature substantially: $\Delta\rho/\rho \approx 0.1$. Since radio waves propagate along the local magnetic field lines, such curvature variations cause changes in the emission direction.

There is unequivocal correspondence between the observable intensity and α (the angle between the observer's line of sight and the emission direction (figure 7)). The maximum of the intensity corresponds to the minimum of α . The period of the pulsar is the time interval between neighbouring maxima of observable intensity (minima of α). Because of this, we can say that the observable period is the representative value of α and, as will be shown below, it might differ from the spin period of the pulsar. Figure 7 shows that

$$\cos \alpha = \mathbf{A} \cdot \mathbf{K}. \quad (66)$$

Here, \mathbf{A} and \mathbf{K} are unit guide vectors of the observer's axis, and the emission axis, respectively. In the spherical coordinate system (r, φ, θ) , combined with plane of pulsar

Table 3. Radio pulsars with long periods.

Number	Pulsar	P (s)	$dP/dt(10^{-15})$	$B_s(10^{12} \text{ G})$	$dE/dt(10^{32} \text{ erg s}^{-1})$
I	PSR J2144-3933	8.5	0.48	2	0.00032
II	PSR J1847-0130	6.7	1275	94	1.7
III	PSR J1814-1744	4.0	743	55	4.7

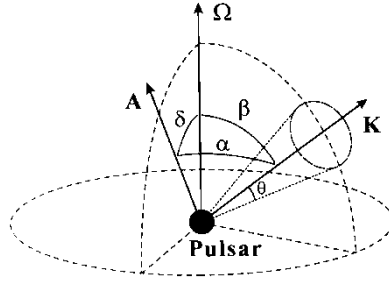


Figure 7. The geometry under consideration. \mathbf{K} is the emission axis; \mathbf{A} is the axis of the observer. The angles δ and θ are constant, while β and α oscillate with time.

rotation, these vectors can be expressed as

$$\mathbf{A} = (1, 0, \delta), \quad (67)$$

$$\mathbf{K} = (1, \Omega t, \beta), \quad (68)$$

where $\Omega = 2\pi/P$ is the angular velocity of the pulsar, δ is the angle between the rotation axis and the observer's axis, and β is the angle between the rotation axis and the emission axis (see figure 7).

From equations (66)–(68) it follows that

$$\alpha = \arccos[\sin \delta \sin \beta \cos(\Omega t) + \cos \delta \cos \beta]. \quad (69)$$

In the absence of the drift wave, $\beta = \beta_0 = \text{constant}$ and consequently the period of α equals $2\pi/\Omega$.

According to equation (65), in the case when the drift wave is present, the fractional variation $\Delta\rho/\rho$ is proportional to the magnetic field B_r of the wave, which changes periodically. So $\beta = \beta(t)$ is harmonically oscillating about β_0 with an amplitude $\Delta\beta = \Delta\rho/\rho$ and rate $\omega_{\text{dr}} = 2\pi/P_{\text{dr}}$. So, we can write

$$\beta = \beta_0 + \Delta\beta \sin(\omega_{\text{dr}} t + \Phi). \quad (70)$$

According to equations (69) and (70), we obtain

$$\begin{aligned} \alpha = \arccos\{ & \sin \delta \sin[\beta_0 + \Delta\beta \sin(\omega_{\text{dr}} t + \Phi)] \cos(\Omega t) \\ & + \cos \delta \cos[\beta_0 + \Delta\beta \sin(\omega_{\text{dr}} t + \Phi)]\}. \end{aligned} \quad (71)$$

The parameters of the pulse profile (*e.g.* the width and the maximum intensity) significantly depend on what would be minimum angle between the emission axis and the observer's axis while the emission axis passes the observer's axis (during 1 rev). If the emission cone does not cross the observer's line of sight entirely, *i.e.* the minimum angle between them is more than the cone angle θ ,

$$\alpha_{\text{min}} > \theta, \quad (72)$$

then pulsar emission is unobservable for us. Contrary to this, the inequality

$$\alpha_{\text{min}} < \theta \quad (73)$$

defines the condition that is necessary for emission detection (figure 8). In this case, the observed pulses must be quite narrow, as seen in the pulsars under consideration. Sometimes

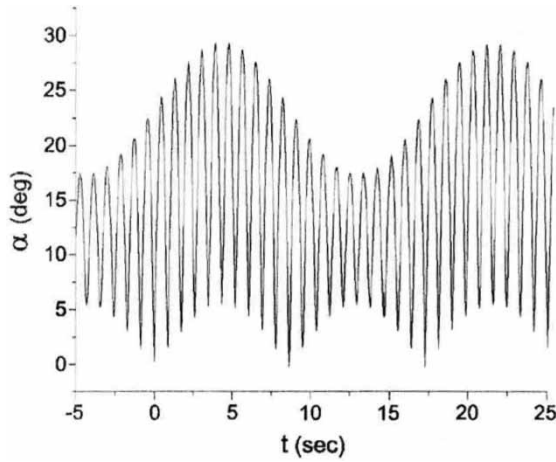


Figure 8. The oscillating behaviour of α with time for $\beta_0 = \delta \approx 0.12$, $\Delta\beta = 0.12$, $\omega_{\text{dr}} = 2\pi/17 \text{ s}^{-1}$, $\Omega = 2\pi/0.85 \text{ s}^{-1}$ and $\Phi = 0$.

we can see several subpulses as a result of subsequent neutron star rotations. Our model predicts the detection of such objects in the future.

Hence for some values of the parameters Ω , ω_{dr} , β , $\Delta\beta$, δ , φ and θ (as the zero point of time reckoning is taken as the detection moment of any pulse) it is possible to accomplish the following regime: after every $k = m$ turn the minimum value of α , denoted α_{min}^m , satisfies condition (73) while, for intervening values of k ($1 \leq k \leq m - 1$, where k and m are positive integers), it satisfies condition (72). In that case the observable period P_{obs} does not represent the real pulsar spin period but is divisible by it:

$$P_{\text{obs}} = mP. \quad (74)$$

It follows from this that

$$\left(\frac{dP}{dt}\right)_{\text{obs}} = m \frac{dP}{dt}. \quad (75)$$

From equations (1), (74) and (75) it follows that

$$B = \frac{B_{\text{obs}}}{m}. \quad (76)$$

After inserting equations (74) and (76) in the equation of the death line of a sunspot configuration field [62] (figure 9),

$$7 \log B_s - 13 \log P = 78, \quad (77)$$

we obtain

$$7 \log B - 13 \log P = (7 \log B_{\text{obs}} - 13 \log P_{\text{obs}}) + 6 \log m \geq 78. \quad (78)$$

Then

$$6 \log m \geq 78 - 7 \log B_{\text{obs}} + 13 \log P_{\text{obs}}. \quad (79)$$

It can be verified that there exists a value for m which satisfies equation (78) and simultaneously the condition

$$B = \frac{B_{\text{obs}}}{m} < B_{\text{cr}}. \quad (80)$$

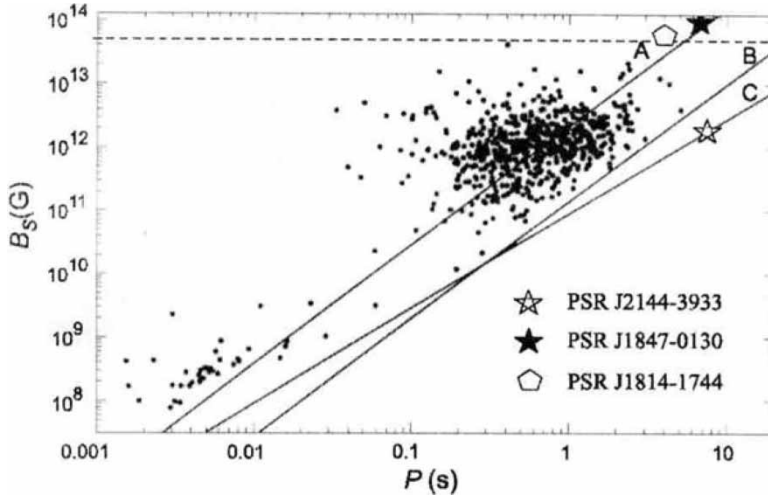


Figure 9. Lines A, B and C are 'death' lines for the dipole magnetic field, the sunspot configuration and the multipolar magnetic field respectively [62]. The broken line represents $B = B_{cr}$. The values of the parameters are taken from table 3.

So, it is possible that there is fulfilment of the conditions necessary for (e^+e^-) pair production for some values of m .

For better estimation of m we can use the observational data for beaming fractions. From figure 7 it appears that the pulse width can be expressed as

$$W = P \frac{2 \sin \theta}{2\pi \sin \delta}. \quad (81)$$

After inserting equation (74) in equation (81), we obtain

$$\frac{mW}{P_{obs}} = \frac{\sin \theta}{\pi \sin \delta}. \quad (82)$$

As was mentioned above, to accomplish the described regime (equation (74)), α_{min}^1 (the angle between the observer's line and the emission direction after 1 rev from that moment when they were coincident, $\alpha = 0$ (figure 7)) must be less than θ :

$$\alpha_{min}^1 = \Delta\beta \sin \left(\frac{2\pi P}{P_{dr}} \right). \quad (83)$$

If we assume that $\beta_0 = \delta$, then we obtain $P_{dr} = 2P_{obs} = 2mP$ and

$$\theta_{max} = \Delta\beta \sin \left(\frac{\pi}{m} \right). \quad (84)$$

If we substitute this equation in equation (82), we obtain

$$\frac{W}{P_{obs}} = \frac{\Delta\beta \sin(\pi/m)}{m\pi \sin \delta}. \quad (85)$$

Here, the left-hand side is known from observations. Equation (85) gives us the ability to estimate the angular parameters of pulsars for a given m .

If we consider all pulsars in the framework of our model, their parameters (spin, magnetic fields, etc.) will obtain new 'real' values, shown in table 3.

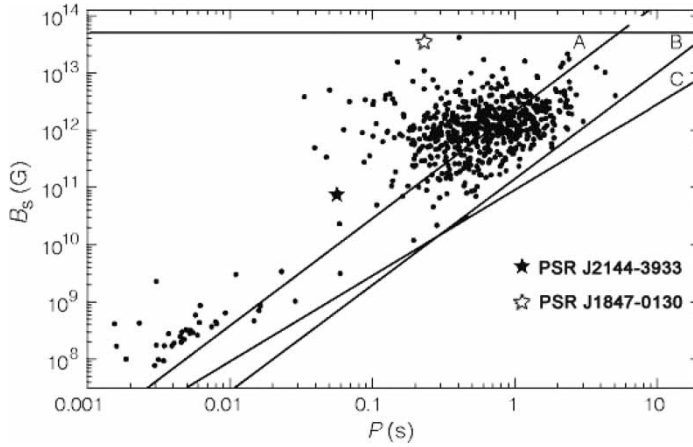


Figure 10. Real positions of the considered pulsars on the $B_s - P$ diagram (table 3).

If we use the observed values of parameters (table 3), the location of pulsars under consideration in the $B_s - P$ diagram are presented in figure 9.

According to the obtained results, the considered pulsars will be placed in the $B_s - P$ diagram as shown in figure 10.

It should be noted that the effect caused by the drift wave (increasing the observational period; see equation (74)) is accomplished only in the case when P_{dr} is divisible by P to a high accuracy (while meeting other additional conditions). In other cases, some interesting effects appear [38]. Thus, we developed the theoretical model of pulsar emission, in the framework of which we explained the main specific features of pulsars presented in table 4.

It should be noted that this model is applicable to all populations of pulsars, but there is a difference in the effects caused by drift waves depending on the values of the parameters. In the case of large $\Delta\beta$ ($\Delta\beta > \theta$) the most interesting effect is the increase in the observable period (see equation (74)) which is accomplished only when P_{dr} is divisible by P to a high accuracy.

In the case of small $\Delta\beta$ ($\Delta\beta < \theta$) there is no increase in the observable period, but some other interesting effects appear, such as drifting subpulses [38], and the period and period derivative oscillation phenomenon, which is observed in PSR B1828-11 [63] and PSR B1642-03 [64]. Some researchers [65–67] have proposed different models to explain this phenomenon within the framework of the free precession of neutron stars. However, as shown by Shaham [21] and Sedrakian *et al.* [22], the existence of free precession in a neutron star is in strong conflict with the superfluid models for the interior structure of a neutron star. Therefore we can state that there no self-consistent explanation of this fact existed.

If P_{dr} is not divisible by P , then the observed intensity must be modulated with the period of the drift wave. It is impossible to obtain such variations with integrated pulse profiles.

Table 4. Revised values of pulsar parameters.

Pulsar	m	P_{dr} (s)	P (s)	$(dP/dt)_{-15}$	B_s (10^{12} G)	dE/dt (10^{32} erg s^{-1})	$\Delta\beta$ (deg)	$\beta_0 \approx \delta$ (deg)	θ (deg)	W_{10}/P
PSR J2144-3933	10	17.0	0.85	0.048	0.2	0.032	7	7	1.5	0.1
PSR J1847-0130	6	13.4	1.12	210	16	61	5	5	3	0.3
PSR J1814-1744	8	8.0	0.5	190	6.9	300	5	5	2	0.2

Deviations of the integrated pulse intensities damp each other. The only possible way to prove this consideration is single pulse observations. Such observations really show intensity variations [68]. Even though they do not have a harmonic nature (this is due to various noises and insufficient resolution), it benefits our model. So, if it is handled so that the oscillating component evolves, this will be one of the best confirmations of our theory.

Let us consider pulsars with very short periods. As was mentioned, drift waves arise in the vicinity of the light cylinder. The shorter the pulsar spin period, the smaller is the radius of the light cylinder and consequently the larger is the magnetic field value in the wave generation region ($B_\varphi \approx B = B_s (R_{*/r})^3$). So, if we take into account this consideration, from equation (65) it follows that the amplitude of oscillation of the emission direction will be so small ($\Delta\beta < 1^\circ$) for those pulsars whose period is less than 0.1 s that the presence of the drift wave does not cause any significant effect.

Generated at different altitudes, radio and higher-frequency synchrotron emissions propagate in different directions. There might be a case such that these two frequencies could be observed with different periodicities. More precisely, the period of X-ray pulsations will be equal to the pulsar spin period, while the radio emission will be modulated with the drift wave period. Even though there are several dozens of known pulsars with multiple wavelengths, none of these has a long period. For this, it seems the other effects mentioned above have to exist. This fact is not surprising if we consider that in all the populations (more than 1000) the number of long-period radio pulsars is only three (see table 3). The discovery of such a pulsar would be another good test of our model.

From these considerations we can divide radio pulsars into the groups listed below, together with their main requirements.

- (i) Rapidly rotating pulsars, for which $\Delta\beta$ is too small: none of the above-mentioned effects should exist for these.
- (ii) Pulsars with $\Delta\beta < \theta$ and $(P_{\text{dr}} - P)/P_{\text{dr}} \ll 1$: in this case, oscillations in the period, period derivative and pulse shape should appear. In the case of low accuracy of equality between P_{dr} and P , subpulse drift can be observed.
- (iii) Pulsars with $\Delta\beta < \theta$: they should show observed intensity variations, which are modulated with the period of the drift waves.
- (iv) Pulsars with $\Delta\beta > \theta$ and $(P_{\text{dr}} - mP)/P \ll 1$ (m is a positive integer): there are differences from the real long observable rotation period.

Thus, long-period radio pulsars represent one of the branches of usual pulsars and must be considered in the framework of traditional theories for the specific values of the parameters.

Recently discovered transient radio pulsars [69] may belong to the population of objects described by our model. Indeed, five of these have rather long visible periods ($P > 4$ s) and one has a surface magnetic field obtained in the magnetodipole model: $B_s = 5 \times 10^{13}$ G $> B_{\text{cr}}$. Precession, star quakes or other reasons can lead to the fulfilment of the condition (73) for a short time and to the appearance of a number of visible pulses.

9. Discussion

One of the main characteristics of the observed emission is the stability of the pulse periods. As we have stated already, the drift waves are stabilized owing to the rotation of the neutron star and the permanent injection of relativistic particles in the region of their generation. Moreover, as was shown by Gogoberidze *et al.* [70], the nonlinear induced scattering leads to a transfer of waves from higher to lower frequencies. As a result, one eigenmode becomes dominant.

So the wave energy accumulates in waves with a certain azimuthal number m , characterizing the lowest frequency. This means that the period of the modulation and the interval between observed pulses must be rather stable.

We have used the suggestion about the small angles between the rotation axes and magnetic moments of neutron stars in AXPs and SGRs. In fact, observed X-ray pulses in these objects are quite wide, and this indicates that they are nearly aligned rotators.

10. Conclusions

- (1) It is shown that there are many difficulties in the magnetar model.
- (2) The drift model is proposed to explain the main peculiarities of AXPs and SGRs.
- (3) In the framework of the drift model, the rotation periods P , their derivatives dP/dt and magnetic fields B in the region of emission generation are calculated for AXPs and SGRs:

$$P = 10\text{--}740 \text{ ms}, \quad \langle P \rangle = 161 \text{ ms},$$

$$\frac{dP}{dt} = 3.7 \times 10^{-16}\text{--}5.5 \times 10^{-12},$$

$$\log B = 2.63\text{--}6.25.$$

- (4) The magnetic fields at the surface of AXPs and SGRs are estimated:

$$\log B_s = 11.22\text{--}13.24,$$

$$\langle \log B_s \rangle = 11.90.$$

- (5) In the drift model, modulation of the emission with periods of the order of 0.1 s should be observed.
- (6) The persistent X-ray emission in the range 1–10 keV can be explained by cyclotron radiation at the surface with magnetic fields $B_s \approx 10^{12}$ G.
- (7) Cyclotron lines can be observed in this diapason.
- (8) If the magnetar model is realized, an absorption line with an energy of the order of 1 MeV must be observed.
- (9) Any cataclysms at the surface of a neutron star in AXPs or SGRs should cause bursts of emission in the X-ray or gamma-ray range with power $2\gamma^2$ times higher than the persistent X-ray value.
- (10) Radio pulsars with observed periods $P > 4$ s can be described in the framework of the drift model too.

Acknowledgement

This work was partly supported by the Russian Foundation for Basic Research (project 03-02-16509) and the National Science Foundation (project 00-98685).

References

- [1] R.C. Duncan and C. Thompson, *Astrophys. J.* **392** L9 (1992).
- [2] M.G. Baring and A.K. Harding, *Astrophys. J.* **507** L55 (1998).
- [3] S. Mereghetti, in *The Neutron Star–Black Hole Connection*, Proceedings of the NATO Advanced Study Institute Series, Series C: Mathematical and Physical Sciences, Vol. 567, edited by C. Kouveliotou, J. Ventura and E. Van den Heuvel, Elounda, Crete, Greece, 7–18 June 1999 (Kluwer, Dordrecht, 2001), p. 351.

- [4] K. Hurley, AIP Conf. Proc. **526** 723 (2000).
- [5] S. Mereghetti, *Proceedings of the Volcano Workshop*, Frontier Objects in Astrophysics and Particle Physics, Ed. F. Giovanelli and G. Mannocchi. Italian Physical Soc., 22–27 May 2000, Italy, p. 239 (2001).
- [6] M.G. Baring and A.K. Harding, *Astrophys. J.* **547** 929 (2001).
- [7] G. Israel, S. Mereghetti and L. Stella, *Mem. Soc. Astron. Ital.* **73** 465 (2002).
- [8] V. Hambarian, G. Hasinger, A.D. Schwöpe *et al.*, *Astron. Astrophys.* **381** 98 (2002).
- [9] D.M. Palmer, S. Barthelmy, N. Gehrels *et al.*, *Astro-ph/0503030* (2005).
- [10] C. Kouveliotou, S. Dieters and T. Strohmayer, *Nature* **393** 235 (1998).
- [11] C. Thompson and R.C. Duncan, *Astrophys. J.* **473** 822 (1996).
- [12] Yu.P. Shitov, V.D. Pugachev and S.M. Kutuzov, in *Pulsar Astronomy – 2000 and Beyond*, IAU Colloquium 177, Astronomical Society of the Pacific Conference Series, Vol. 202, edited by M. Kramer, N. Wex and N. Wielebinski Astronomy Society of the Pacific, San Francisco, USA (2000), p. 685.
- [13] V.M. Malofeev, O.I. Malov, D.A. Teplykh *et al.*, *Astron. Rep.* **49** 242 (2005).
- [14] D. Marsden, R.E. Lingefelter, R. E. Rothschild *et al.*, *Astrophys. J.* **550** 387 (2001).
- [15] I.F. Malov, *Astron. Lett.* **29** 502 (2003).
- [16] X.-D. Li, *Astrophys. J.* **520** L271 (1999).
- [17] B. Paczynski, *Astrophys. J.* **365** L9 (1990).
- [18] V. Usov, *Astrophys. J.* **410** 761 (1993).
- [19] A. Dar and De Rujula, *Results and Perspectives in Particle Physics*, Vol. XVII, edited by M. Greco, La Thule, Aosta Valley, p. 13 (2000).
- [20] V.V. Usov, *Phys. Rev. Lett.* **87** 1001 (2001).
- [21] J. Shaham, *Astrophys. J.* **214** 251 (1977).
- [22] A. Sedrakian, I. Wasserman and J.M. Cordes, *Astrophys. J.* **524** 341 (1999).
- [23] G.Z. Machabeli and V.V. Usov, *Soviet Astron. Lett.* **5** 238 (1979).
- [24] D.G. Lominadze, G.Z. Machabeli and A.B. Mihailovskii, *Fiz. Plazmy* **5** 1337 (1979).
- [25] A.Z. Kazbegi, G.Z. Machabeli, G.I. Melikidze *et al.*, *Proceedings of the Joint Varenna–Abastumani International School and Workshop on Plasma Astrophysics*, Vol. 1 European Space Agency, Paris, 1989), p. 271.
- [26] A.Z. Kazbegi, G.Z. Machabeli and G.I. Melikidze, in *Magnetospheric Structure and Emission Mechanics of Radio Pulsars*, IAU Colloquium 128, edited by T. H. Hankins, J. M. Rankin and J. A. Gil (Pedagogical University Press, 1992), Zielona Gora, Poland, p. 232.
- [27] M. Lyutikov, G.Z. Machabeli and R. Blandford, *Astrophys. J.* **512** 804 (1999).
- [28] M. Lyutikov, R. Blandford and G.Z. Machabeli, *Mon. Not. R. Astron. Soc.* **305** 358 (1999).
- [29] I.F. Malov and G.Z. Machabeli, *Astrophys. J.* **554** 587 (2001).
- [30] J. Arons, *Proceedings of the International Summer School and Workshop on Plasma Physics*, edited by T.D. Guyenne (European Space Agency, Paris, 1981), p. 273.
- [31] A.S. Volokitin, V.V. Krasnosel'skikh and G.Z. Machabeli, *Fiz. Plazmy* **11** 310 (1985).
- [32] J. Arons and J.J. Barnard, *Astrophys. J.* **302** 120 (1986).
- [33] A.Z. Kazbegi, G.Z. Machabeli, G.I. Melikidze *et al.*, *Astron. Astrophys.* **309** 515 (1996).
- [34] G.Z. Machabeli, Q. Luo, D. Melrose *et al.*, *Mon. Not. R. Astron. Soc.* **312** 51 (2000).
- [35] G.Z. Machabeli, Q. Luo, S. Vladimirov *et al.*, *Phys. Rev.* **65** 6408 (2002).
- [36] A.Z. Kazbegi, G.Z. Machabeli and G.I. Melikidze, *Aust. J. Phys.* **44** 573 (1987).
- [37] O. Chedia, J. Lominadze, G. Machabeli *et al.*, *Astrophys. J.* **479** 313 (1997).
- [38] G.Z. Machabeli, D. Khechinashvili, G.I. Melikidze *et al.*, *Mon. Not. R. Astron. Soc.* **327** 984 (2001).
- [39] I.F. Malov and G.Z. Machabeli, *Astron. Rep.* **46** 684 (2002).
- [40] I.F. Malov, G.Z. Machabeli and V.M. Malofeev, *Astron. Rep.* **47** 232 (2003).
- [41] I.F. Malov, *Astron. Rep.* **45** 389 (2001).
- [42] F.P. Gavriil and V.M. Kaspi, *Astrophys. J.* **567** 1067 (2002).
- [43] I.F. Malov, *Astron. Rep.* **50** 398 (2006).
- [44] A. Possenti, R. Cerutti, M. Colpi *et al.*, *Astron. Astrophys.* **387** 993 (2002).
- [45] P.M. Woods and C. Thompson, *Astro-ph/0406133* (2004).
- [46] G. Hobbs, R. Manchester, A. Teoh *et al.*, *Astro-ph/039219* (2003).
- [47] A.F. Illarionov and R.A. Sunyaev, *Astron. Astrophys.* **39** 185 (1975).
- [48] R.V.E. Lovelace, M.M. Romanova and G.S. Bisnovaty-Kogan, *Astrophys. J.* **514** 368 (1999).
- [49] L.-D. Zhang, Q.-H. Peng and X.-L. Luo, *Chin. Phys. Lett.* **20** 1175 (2003).
- [50] I.F. Malov, *Astron. Rep.* **48** 337 (2003).
- [51] I.F. Malov and O.I. Malov, *Astron. Rep.* **50** 483 (2006).
- [52] L.D. Landau and E.M. Lifshitz, *Classical Theory of Fields* (Pergamon, London, 1971).
- [53] L.D. Landau and E.M. Lifshitz, *Quantum Mechanics* (Fizmatgiz, Moscow, 1963).
- [54] N. Rea, G.L. Izrael and L. Stella, *Nucl. Phys. B, Proc. Suppl.* **132** 554 (2004).
- [55] S. Zane, R. Turrolo, L. Stella *et al.*, *Astrophys. J.* **560** 384 (2001).
- [56] W.C.G. Ho, D. Lai, A.Y. Potekhin *et al.*, *Adv. Space Res.* **33** 537 (2004).
- [57] G. Bekefi, *Radiation Processes in Plasmas*, edited by G. Bekefi (Wiley, New York, 1966).
- [58] M.D. Young, R.N. Manchester and S. Johnston, *Nature* **400** 848 (1999).
- [59] M.A. McLaughlin, J.H. Stairs, V.M. Kaspi *et al.*, *Astrophys. J.* **591** L135 (2003).
- [60] F. Camilo, V.M. Kaspi, A.G. Lyne *et al.*, *Astrophys. J.* **541** 367 (2000).
- [61] D. Lomiashvili, G. Machabeli and I. Malov, *Astrophys. J.* **637** 1010 (2006).

- [62] K. Chen and M.A. Ruderman, *Astrophys. J.* **402** 264 (1993).
- [63] I.H. Stairs, A.G. Lyne and S. Shemar, *Nature* **406** 484 (2000).
- [64] T.V. Shabanova, A.G. Lyne and J. Urama, *Astrophys. J.* **552** 321 (2001).
- [65] D.I. Jones and N. Andersson, *Mon. Not. R. Astron. Soc.* **324** 811 (2001).
- [66] B. Link and R.I. Epstein, *Astrophys. J.* **556** 392 (2001).
- [67] V. Reznia, *Astron.Astrophys.* **399** 653 (2003).
- [68] A. Karastergiou *et al.*, *Astron.Astrophys.* **379** 270 (2001).
- [69] M.A. McLaughlin, A.G. Lyne, D.R. Lorimer *et al.*, *Astro-ph/ 0511587* (2005).
- [70] G. Gogoberidze, G.Z. Machabeli, D.B. Melrose *et al.*, *Mon. Not. R. Astron. Soc.* **360** 669 (2005).